The α-to-β Conformational Transition of Alzheimer's Aβ-(1–42) Peptide in Aqueous Media is Reversible: A Step by Step Conformational Analysis Suggests the Location of β Conformation Seeding

Simona Tomaselli,[a, b] Veronica Esposito,[a] Paolo Vangone,[a] Nico A. J. van Nuland,[c, d] Alexandre M. J. J. Bonvin,[c] Remo Guerrini,[e] Teodorico Tancredi,[f] Piero A. Temussi,[a, g] and Delia Picone*[a]

Current views of the role of β-amyloid (Aβ) peptide fibrils range from regarding them as the cause of Alzheimer's pathology to having a protective function. In the last few years, it has also been suggested that soluble oligomers might be the most important toxic species. In all cases, the study of the conformational properties of Aβ peptides in soluble form constitutes a basic approach to the design of molecules with "antiamyloid" activity. We have experimentally investigated the conformational path that can lead the Aβ-(1–42) peptide from the native state, which is represented by an α helix embedded in the membrane, to the final state in the amyloid fibrils, which is characterized by β-sheet structures. The conformational steps were monitored by using CD and NMR spectroscopy in media of varying polarities. This was achieved by changing the composition of water and hexafluoroisopropanol (HFIP). In the presence of HFIP, β confor-mations can be observed in solutions that have very high water content (up to 99% water; v/v). These can be turned back to α helices simply by adding the appropriate amount of HFIP. The transition of Aβ-(1–42) from α to β conformations occurs when the amount of water is higher than 80% (v/v). The NMR structure solved in HFIP/H$_2$O with high water content showed that, on going from very apolar to polar environments, the long N-terminal helix is essentially retained, whereas the shorter C-terminal helix is lost. The complete conformational path was investigated in detail with the aid of molecular-dynamics simulations in explicit solvent, which led to the localization of residues that might seed β conformations. The structures obtained might help to find regions that are more affected by environmental conditions in vivo. This could in turn aid the design of molecules able to inhibit fibril deposition or revert oligomerization processes.

Introduction

Extracellular proteic plaques found in the brains of patients affected by Alzheimer's disease contain fibrils composed of β-amyloid (Aβ) peptides. These range in length from 39 to 43 amino acids,[1] the most abundant form being Aβ-(1–42). Although there is evidence of the presence of aggregates inside affected neurons in other neurodegenerative diseases,[2] in the

[a] Dr. S. Tomaselli, V. Esposito, P. Vangone, Prof. P. A. Temussi, Prof. Dr. D. Picone
Dipartimento di Chimica, Università Federico II di Napoli
Via Cintia, 80126 Napoli (Italy)
Fax: (+39) 081-674409
E-mail: delia.picone@unina.it

[b] Dr. S. Tomaselli
Istituto di Biostrutture e Bioimmagini, CNR
Dipartimento di Chimica Biologica, Università Federico II di Napoli
80126 Napoli (Italy)

[c] Dr. N. A. J. van Nuland, Dr. A. M. J. J. Bonvin
Bijvoet Center for Biomolecular Research
Department of NMR Spectroscopy, Utrecht University
Padualaan 8, 3584 CH Utrecht (The Netherlands)

[d] Dr. N. A. J. van Nuland
Current address:
Departamento de Química Física, Facultad de Ciencias
Universidad de Granada, Campus Fuentenueva s/n
18071 Granada (Spain)

[e] Dr. R. Guerrini
Dipartimento di Scienze Farmaceutiche
Università di Ferrara, via Fossato di Mortara 17–19
44100 Ferrara (Italy)

[f] Dr. T. Tancredi
ICB del CNR
via Campi Flegrei 34, 80078 Pozzuoli (Italy)

[g] Prof. P. A. Temussi
Centro Linceo "Beniamino Segre", Accademia dei Lincei
Palazzo Corsini, 00165 Roma (Italy)

Supporting information for this article is available on the WWW under http://www.chembiochem.org or from the author.

case of Alzheimer's disease the toxicity of aggregates—usually connected with the adverse effects of the disease—is particularly difficult to understand since the plaques are external to the neurons. Accordingly, aggregates cannot possibly interfere directly with cell metabolism.[3] A trivial explanation is that by covering a large cell surface, the plaques hinder cellular exchanges with the extracellular environment. Yet another possibility is that fibril formation is driven by lipid-induced aggregation at the membrane surface that is caused by other pathological conditions.[4] More specifically, it has been suggested that membrane damage is caused by oxidative stress from free radicals,[5] or that amyloid plaques could act as large reservoirs of species in equilibrium with neurotoxic oligomers.[6] In the last few years, it has been shown that soluble oligomers might be more important pathologically than fibrillar-amyloid deposits.[7–9] A specific mechanism for the toxicity of oligomeric assemblies was suggested by solution studies of isolated Aβ fragments. The surprising similarity of the Aβ-(1–42) structure in apolar environments to that of a virus fusion peptide[10] points to membrane poration as the key event for neurotoxicity. The α-helical peptide could induce formation of membrane channels, thereby allowing the penetration of substances (such as metal ions) that can cause neuronal death.[9, 11, 12] Recently, different structures of aggregated forms, the so-called β-balls, have also been proposed.[13]

Irrespective of the details of each mechanism, most views on neurotoxicity evidence a critical role for in vivo conformational transitions between soluble α helical and β forms of the peptide. Direct observation of such conformational transitions is difficult since all Aβ peptides have little tendency to dissolve in water. Furthermore, when transferred from organic solvents to aqueous solutions, they show a great propensity to aggregate and eventually precipitate. NMR investigations on small Aβ fragments[14–16] and Aβ-(1–40)^{ox}[17] suggest that in aqueous solution Aβ peptides can be described as random coils, with only a small population of local nonrandom structures.[14] Overall, there is a strong indication that neat water is not suitable for high-resolution conformational analysis of Aβ peptides. Accordingly, detailed structural studies are normally performed in mixtures of water and organic solvents, particularly fluorinated alcohols, such as trifluoroethanol (TFE) or hexafluoroisopropanol (HFIP), and micellar solutions.[10, 15–21] In these media, Aβ peptides are not aggregated and have predominantly α-helical conformations.

An interesting possibility for monitoring the α-to-β transition was suggested by the observation that, in addition to promoting α helices, mixtures of water and TFE can induce β structure in narrow concentration ranges. This was demonstrated by Barrow and Zagorski[18] and Otvos et al.[22] for Aβ-(1–42) mainly by using CD spectroscopy. In the concentration range from 10 to 32.5% of TFE (v/v), Aβ-(1–42) forms β-sheet structures, whereas in the concentration range 50–100% TFE CD spectra are typical of α-helices. However, early precipitation of aggregates from β structures in vitro has so far prevented the observation of reversible transitions and characterization of intermediate structures with sufficient detail.

Mixtures of HFIP/H$_2$O seemed more promising than those of TFE/H$_2$O for these studies. We have recently studied the conformational properties of Aβ-(1–42) in several media that can create apolar microenvironments that mimic the lipid phase of membranes. A structure of unprecedented detail was obtained by using a HFIP/H$_2$O 80:20 (v/v) aqueous mixture.[10] We deem that this structure could represent an ideal starting point for monitoring environment-induced conformational transitions. In addition, the unique properties of HFIP offer the opportunity to tune the polarity of the medium at concentrations suitable for NMR studies[10] while keeping Aβ-(1–42) in solution, and to study the peptide in mixtures that have very high water content. Mixtures of gradually varying polarity were used to monitor reversible conformational transitions of Aβ peptide from helical to β forms, and the structure of Aβ-(1–42) in a mixture with very high water content was determined. We followed the conformational transitions using an integrated approach of experimental and theoretical methods. Conformations of helical forms found in the concentration range of 10 to 80% water were determined at the atomic level by NMR spectroscopy. However, β conformations present in the range of 90–99% water, were followed by CD spectroscopy. These conformations are stable for extended periods of time and can be turned back to α helices by addition of appropriate amounts of HFIP—even starting from solutions that contain as much as 99% water. Conformational equilibria that affected the transition were described by molecular dynamics (MD) simulations. These studies hint at likely nucleation points for the formation of β conformations.

Results

Conformations in mixtures with very high water content

The main goal of our work is to investigate experimentally the conformational path that can lead the Aβ-(1–42) peptide from the native state (represented by an α helix embedded in the membrane) to the final state in amyloid fibrils (characterized by β-sheet structures). Furthermore, we want to suggest the most likely traits in the sequence that can initiate the α-to-β conformational transition. We have previously shown that HFIP/H$_2$O mixtures favor the helical propensity of Aβ-(1–42) more strongly than those of TFE/H$_2$O.[10] Preliminary work with CD spectroscopy showed that it was possible to increase the percentage of water in HFIP to very high values if it was done gradually and with extreme care. With the aim of evaluating the effect of more-polar media on the conformational properties of the peptide, we performed a CD spectroscopy study of Aβ-(1–42) in mixtures of water and HFIP. We systematically increased the water content from 60% (v/v), which corresponds to a molar fraction of 0.897, up to 99%, which corresponds to a molar fraction of 0.998. Figure 1 shows experimental CD spectra of freshly prepared Aβ-(1–42) solutions in mixtures that vary from 60% to 90% water, together with calculated spectra derived from a combined analysis carried out with the CONTIN and CDSSTR programs.[23] The spectra clearly indicate that the peptide retains a mainly helical conformation in up to 80%
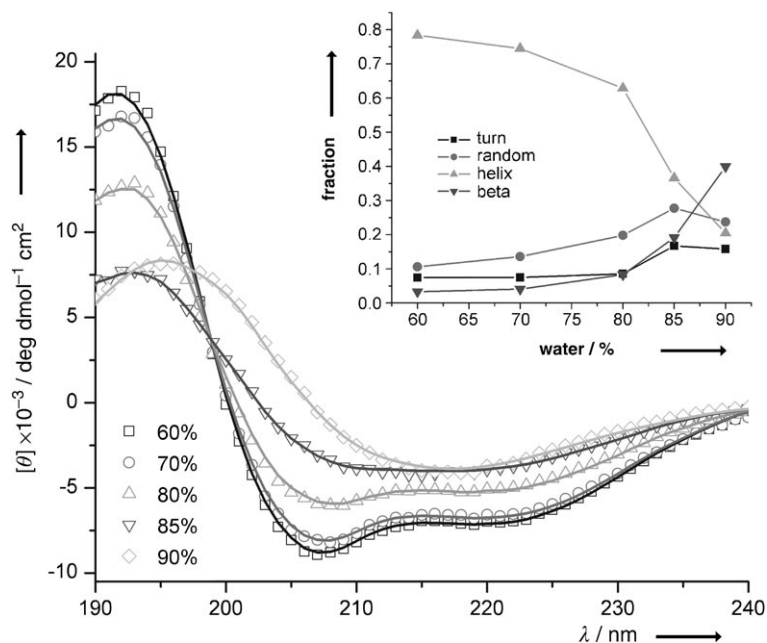
Figure 1. CD spectra of freshly prepared solutions of Aβ-(1–42) in different HFIP/H$_2$O mixtures. The amount of water varies from 60 to 90%, which corresponds to molar fractions ranging from 0.897 to 0.981. Experimental data points are shown as symbols; calculated spectra that were derived from a combined analysis by using CONTIN and CDSSTR (see Experimental Section) are shown as solid lines. The inset shows the fraction of turn, random (unordered), helix (regular + distorted), and β (regular + distorted) conformations in different percentages of water, obtained from the combined analysis.

water, and becomes primarily β structured at 90% water content. The inset in Figure 1 shows that in up to 80% water the helical content gradually decreases with a concomitant increase in both random and β structures. The sharp transition from helical to β conformation is at around 85% water. These observations are similar to those described for TFE/H$_2$O[24] and HFIP/H$_2$O[25] mixtures, with two significant differences: in HFIP/H$_2$O, the conformational transition was more cooperative (the transition region of the curve is steeper in Figure 1, inset); most of all, however, all solutions, including the ones with 90% water, proved to be very stable, as the CD spectra did not change over months.

Reversibility of the transition

In the presence of HFIP, the amount of water can be increased even above 90% before precipitation of aggregates is observed. Moreover, Aβ-(1–42) conformation in a given medium can be easily shifted toward α helix or β sheet by simply changing the solvent composition by the addition of either HFIP or water, respectively. This can be used to probe the influence of environmental conditions at the extremes of the polarity range on conformational equilibria. Figure 2 A shows the variations in CD spectra during the change from a partially helical state, which is typical of the beginning of the α-to-β transition (HFIP/H$_2$O, 20:80, spectrum a), to a completely β structure (HFIP/H$_2$O, 1:99, spectrum b), and back to a fully structured state (HFIP/H$_2$O, 80:20, spectrum c). In order to maintain the

same peptide concentration (50 μM), the three samples in Figure 2 A were prepared by diluting a 1 mM stock solution of Aβ-(1–42) in HFIP/H$_2$O 20:80 with the appropriate solvent mixture. As expected, spectra in mixtures that contained 20% (spectrum a) and 99% (spectrum b) water had profiles that were typical of α-helical and β-sheet structures, respectively. The molar ellipticity of spectrum c (HFIP/H$_2$O, 80:20) is higher and reflects the higher content of secondary structure in the less polar environment. It is important to stress that, although the composition of the 1:99 HFIP/H$_2$O solution (spectrum b) is very close to that of neat water (molar fraction 0.998), the presence of 0.2% HFIP is sufficient to stabilize the β conformation and keep the peptide stable for several hours. Figure 2 B shows the effect of time dependence combined with solvent composition. Spectrum d in Figure 2 B coincides with spectrum b of Figure 2 A (Aβ-(1–42) in HFIP/H$_2$O, 1:99). After 72 h, there was considerable loss of intensity (Figure 2 B, spectrum e) but no visible precipitate was observed, even during the following three weeks (data not shown). Moreover, even a peptide dissolved in this almost completely aqueous environment can be turned back to an α-helix simply by adding the appropriate amount of HFIP. Spectrum f in Figure 2 B shows the sample from spectrum e after addition of HFIP to obtain a solution of Aβ-(1–42) in HFIP/H$_2$O 80:20: the peptide again adopted an essentially α-helix conformation. Furthermore, spectrum g of the same sample, which was recorded seven days later, had a very similar shape but higher intensity. This indicates that the conversion of β aggregates into the α conformation takes place at a very low rate. The possibility to switch the peptide conformation reversibly by varying the solvent composition was also confirmed by 1D NMR spectroscopy (data not shown). Thus, the HFIP/H$_2$O mixtures represent a versatile, suitable medium for following the conformational transition from the soluble, helical form described previously[10] to the extended structure described here.

Exploring the transition region at atomic detail

NMR is well suited for detailed structural determinations, but it was not possible to characterize the β structures of Aβ-(1–42) in HFIP/H$_2$O when water content was higher than 85%. At peptide concentrations typically used for NMR spectroscopy, which are much higher than those necessary for CD spectroscopy, the peptide precipitated. Nonetheless, it proved possible to use NMR spectroscopy in a qualitative fashion to monitor the conformational transitions induced by increasing solvent polarity. Figure 3 shows the low-field regions of 1D NMR spectra of Aβ-(1–42) in HFIP/H$_2$O mixtures that had water contents varying from 20% to 99%. It is highly significant that 1D NMR spectra acquired from HFIP/H$_2$O 80:20 (Figure 3 A) up to 20:80 mixtures (Figure 3 B) did not display significant differences. This implies that even in media in which Aβ-(1–42) is at its transition point, its conformation is similar to that obtained in

A)

B)
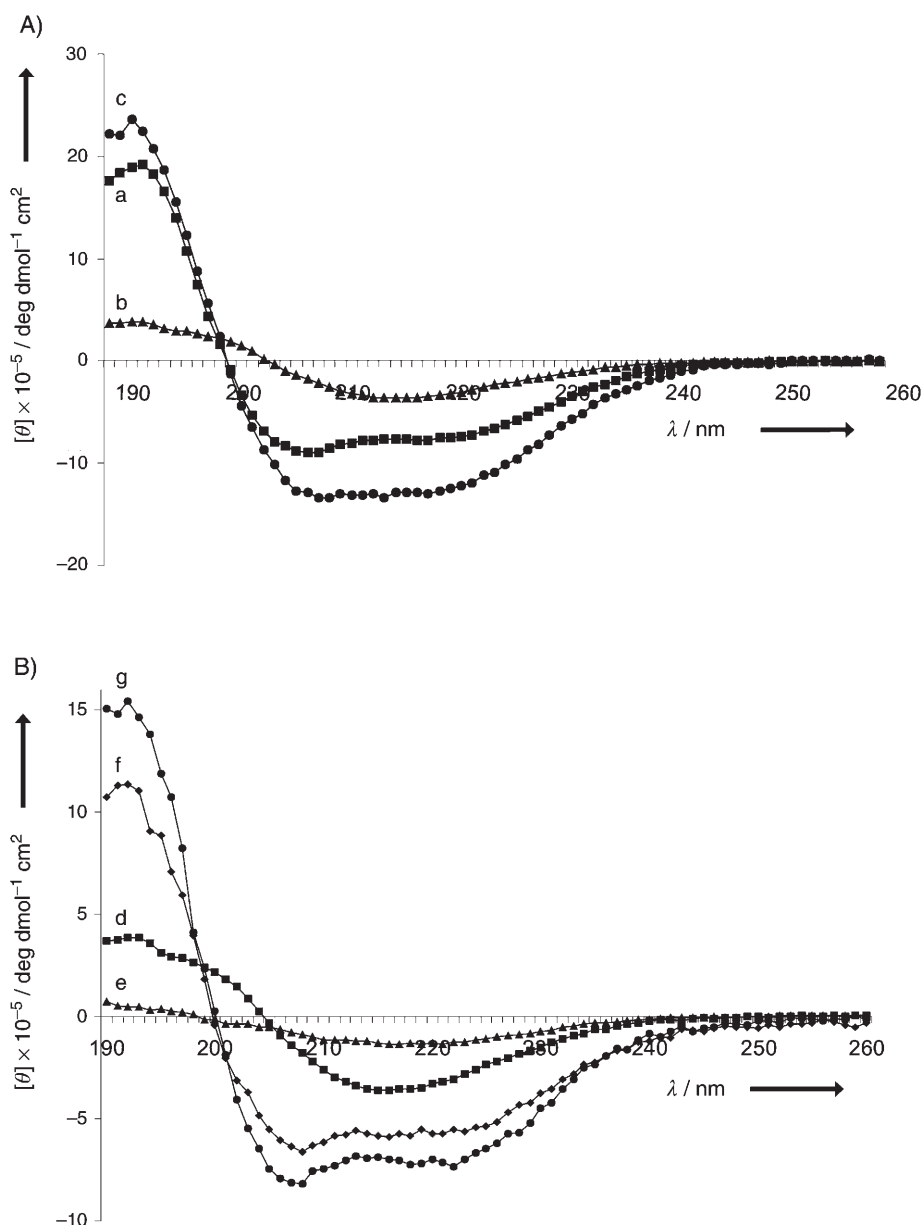
Figure 2. A) CD spectra showing the variations observed on going from a) a partially helical state (HFIP/H$_2$O 20:80; to b) a completely β structure (HFIP/H$_2$O 1:99; and c) back to a fully structured state (HFIP/H$_2$O 80:20). B) Time and solvent dependence. d) CD spectra of Aβ-(1–42) in a freshly prepared HFIP/H$_2$O 1:99 mixture; e) spectrum of the same sample after 72 h; f) spectrum of sample e after addition of HFIP to obtain a HFIP/H$_2$O 80:20 mixture; g) spectrum of sample f after seven days.

detail, as was revealed by CD spectroscopy. The low resolution and the clear evidence of aggregation in solutions with water content equal to or higher than 90% makes the elucidation of a 3D structure by NOE-based methods practically impossible. Therefore, we sought to characterize the conformational state before the transition with as much structural detail as was possible, that is, we used media in which the peptide was as close to transition between α and β conformations as possible.

In order to determine the highest water concentration that resulted in ordered conformations in the vicinity of the transition point indicated by CD analysis (85% water), we performed extensive qualitative analysis of chemical shifts. By comparing NH chemical shifts obtained under different experimental conditions (60, 70, and 80% water) with the reference sample (20% water), we observed substantial differences in the C-terminal region, except for residues 33–36. However, the interpretation of these data is not straightforward, since it is difficult to discriminate between conformational and solvation effects. On the other hand, chemical-shift deviations from random-coil values can reveal traits of secondary structure. Strictly speaking, analysis of the chemical-shift deviations requires knowledge of random-coil shifts under all experimental conditions explored, particularly for amide-proton chemical shifts that can undergo

mixtures that are much richer in the organic component—in particular the HFIP/H$_2$O 80:20 mixture, in which the peptide is in its fully structured state.[10] The limited spread of the amide chemical shifts confirmed the prevalent helical character indicated by CD analysis under these experimental conditions. The 1D spectra corresponding to HFIP/H$_2$O 10:90 and 1:99 (Figure 3C and D, respectively), which display features typical of a more disordered state, show that, even at a very low peptide concentration, some aggregation is present. Obviously, it is not possible to pinpoint the resonances originating from the few residues that assume a β conformation in these mixtures in

specific solvation by HFIP. However, if we are only interested in the trend of conformational preferences as a function of mixture composition, it might be sufficient to use literature values for aqueous solutions. By using random-coil values for NH resonances reported either by Wüthrich[26] or Wishart and Sykes,[27] chemical shifts of the mixtures explored (60, 70, and 80% water, *v/v*) show that, as the percentage of water is increased, helicity in the N-terminal part of Aβ peptide is essentially preserved. However, the C-terminal part is always more disordered (data not shown). A more reliable comparison can be performed by measuring Cα chemical-shift deviation from
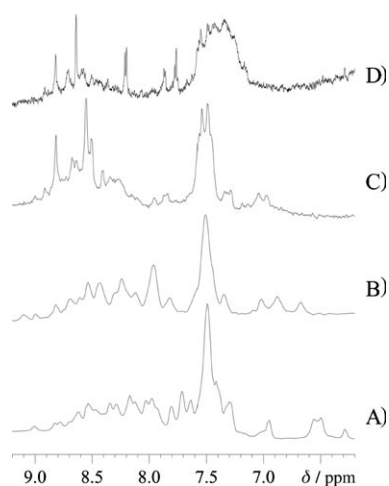
Figure 3. Conformational transition of Aβ-(1–42) as monitored by ^{1}H 1D NMR spectroscopy. Low-field regions of 1D NMR spectra of Aβ-(1–42) in HFIP/H$_2$O mixtures, with water contents ranging from 20 to 99%. A) ^{1}H 1D NMR spectrum at 600 MHz in HFIP/H$_2$O 80:20; B) ^{1}H 1D NMR spectrum at 600 MHz in HFIP/H$_2$O 20:80; C) ^{1}H 1D NMR spectrum at 600 MHz in HFIP/ H$_2$O 10:90; D) ^{1}H 1D NMR spectrum at 600 MHz in HFIP/H$_2$O 1:99.

random-coil values, since these resonances are less affected by solvation and should reflect genuine conformational effects. Comparison between values of mixtures with 70 and 20% water content (Figure 4 A and B, respectively) further indicates that the conformational state of Aβ peptide is quite similar in the two media. In conclusion, all three solutions have NMR spectra that are consistent with high helical content, and the 70% solution (the highest water content) still shows data that are amenable to a detailed structural analysis. We realized that, at this percentage of water, it is possible to pinpoint the region of the peptide that changes conformation since in this solution both the CD (Figure 1) and ^{1}H chemical-shift analyses already show a decrease in helical content.

## A helical structure in 70% water solution

It is interesting to note that the molar water fraction (0.929) of the 70% water solution is so high that the results can be considered to be representative of aqueous solutions that are compatible with prevalently helical conformations. In order to give an idea of the quality of the experimental data the fingerprint region of the NOESY spectrum acquired at 750 MHz in 30:70 HFIP/H$_2$O at 300 K is reported in the Supporting Information. Most of the spin systems were easily recognized by comparison with spectra acquired with the 80:20 HFIP/H$_2$O sample. However, all backbone-proton assignments were confirmed by the standard NOE-based sequential-assignment approach. The assignment of the backbone amide-proton resonances was 98% complete since the Gly9 signals were missing from all the spectra acquired. This is probably due to the strong overlap that was observed under all the experimental conditions explored. The chemical shifts are also given as Supporting Information and have been deposited in the PDB under the ID code 1Z0Q.

The bar diagrams summarize the main diagnostic effects derived from NMR spectra and show the prevalence of the typical contacts of helical structures (Figure 4 C and D; many α$_i$-NH$_{i+3}$ and α$_i$-β$_{i+3}$ NOEs). However, the simultaneous presence of strong α$_i$-NH$_{i+1}$ and β$_i$-NH$_{i+1}$ NOEs, which are typical of an extended structure, indicate the presence of a certain disorder over the whole molecule. We performed a full structure calculation in order to characterize the predominant conformer and to define regions whose conformations are more affected by the polar environment. Several DYANA runs were performed on the basis of 100 starting random structures and with 426 NOE restraints (intra = 238, seq = 108, med = 80). These yielded the 30 final conformers shown in Figure 5 A. It is worth noting that the NOEs are not uniformly distributed along the sequence. In comparison with the 10–23 region (intra = 84, seq = 44, med = 48; corresponding to 12.6 NOEs per residue), we observed a lower number of NOEs for the 28–38 region (intra = 73, seq = 29, med = 16; corresponding to 10.7 NOEs per residue). Moreover, despite the adequate number of total NOEs (~10 NOEs per residue), the target functions of the 20 selected conformers were rather high. This reflects an intrinsic degree of disorder in the final structure. According to the NOE distribution, analysis of the ensemble of structures shows that the most structured region corresponds to the 10–23 segment. This region is in an α-helical conformation that has a backbone root mean square deviation (rmsd) value of 1.67 Å. As shown in Figure 5, the 28–38 region, which in the 80:20 mixture was also a regular helix,[10] became much more disordered in HFIP/ H$_2$O 30:70 (v/v). However, a careful analysis of ϕ and ψ angles indicated that the 34–38 region retained a certain degree of helical structure. As far as region 25–28 is concerned, the structural features of the β turn we found in the 80:20 mixtures were present only in a few structures of the ensemble. Table 1 summarizes the relevant statistical data for the structure calculated in the 30:70 mixture in comparison with those previously solved in HFIP/H$_2$O 80:20.

A word of caution is in order when assessing the relevance of this structure. The peptide concentration used to determine the NMR structure in the 30:70 mixture (1 mM) was necessarily much higher than that used to monitor the whole α-to-β transition by CD spectroscopy (16 μM). However, since the helical content of the NMR structure correlates very well with the corresponding CD spectrum in the same solvent, it is fair to assume that also the location of the helical trait corresponds to the actual situation at low concentration.

MD simulations tie CD and NMR spectroscopy data

Detailed experimental characterization of the transition from a fully helical to fully β conformation was hampered by the practical difficulty of observing all steps with a high-resolution technique, such as NMR spectroscopy. In order to identify the regions of the peptide that promote conformational transition and eventually go into β conformation, we resorted to an exhaustive MD calculation. Simulations with GROMACS,[28,29] starting from the accurate NMR structure of Aβ-(1–42), which was previously determined in an apolar environment, were run for

A)

B)

C)

D)
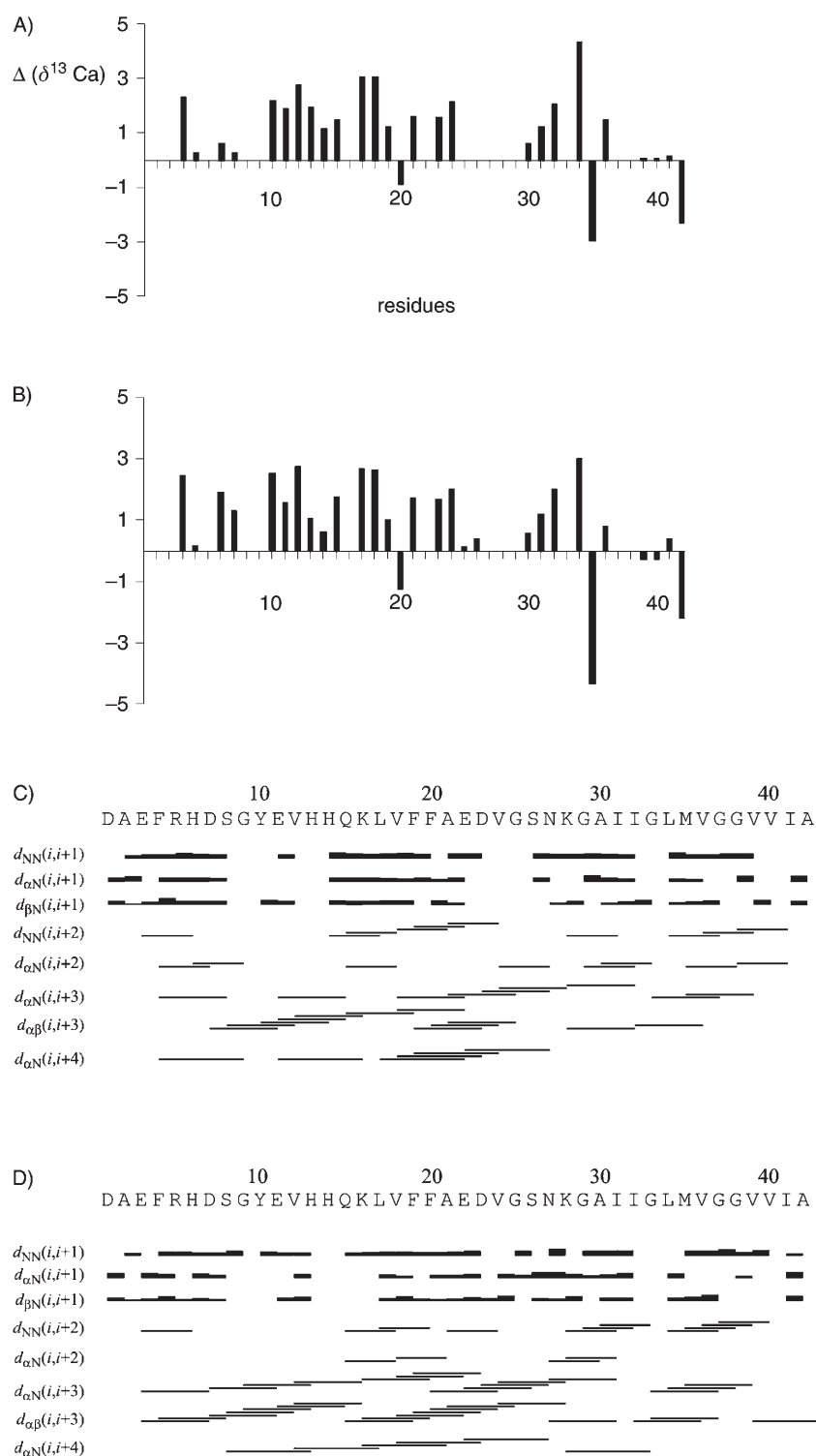
Figure 4. Difference between experimental Cα chemical shifts in A) HFIP/H$_2$O 30:70 and B) HFIP/H$_2$O 80:20, with respect to random-coil values in water and TFE, respectively. Bar diagrams summarizing the main diagnostic effects derived from NMR spectra in C) HFIP/H$_2$O 30:70 and D) HFIP/H$_2$O 80:20; the latter corresponds to the reference solution. The lines' thickness is related to the strength of the NOEs.

in-house scripts, revealed significant changes in secondary-structure elements.

During the long MD simulations, the secondary-structure content was calculated at regular intervals, so that each type could be monitored independently as a function of time. The results are best illustrated by the snapshots shown in Figure 6. The time course at 300 K indicates that immersion of the structure obtained in 20% water[10] into full water induces only a partial destabilization. As shown by Figure 6A, the most affected segment is the C-terminal region, which essentially loses its helical character, except for the central part. It is fair to say that the time evolution at 300 K is in substantial agreement with the NMR structure determined in 70% water. In fact, a detailed analysis of the geometry showed typical α-helical φ and ψ angles for residues 34–38. On the other hand, throughout the simulation the N terminus showed an α-helical conformation for residues that span His10 to Ala21. There was only a slight destabilization in NMR results; this indicates that an α helix spans the whole stretch from Tyr10 to Asp23.

On the other hand, when the temperature was raised to 340 K, analysis of the trajectories revealed the appearance of a β sheet that was formed by two distal β strands. It is interesting to note that the two emerging β strands are located in the central part of the sequences that host the two main helices in the low-polarity structure of Aβ-(1–42).[10] Figure 6B clearly indicates a very dynamic and fluctuating structure at 340 K. The α-helical character of both regions is lost in the first 10 ns, while small stretches of β-structure that involve residues 18–22 and 37–41 begin to appear. Structural details were monitored by calculating the average Cα–Cα distance map that corresponds to the last 20 ns of Aβ-(1–42) MD simulation in water at 340 K (data
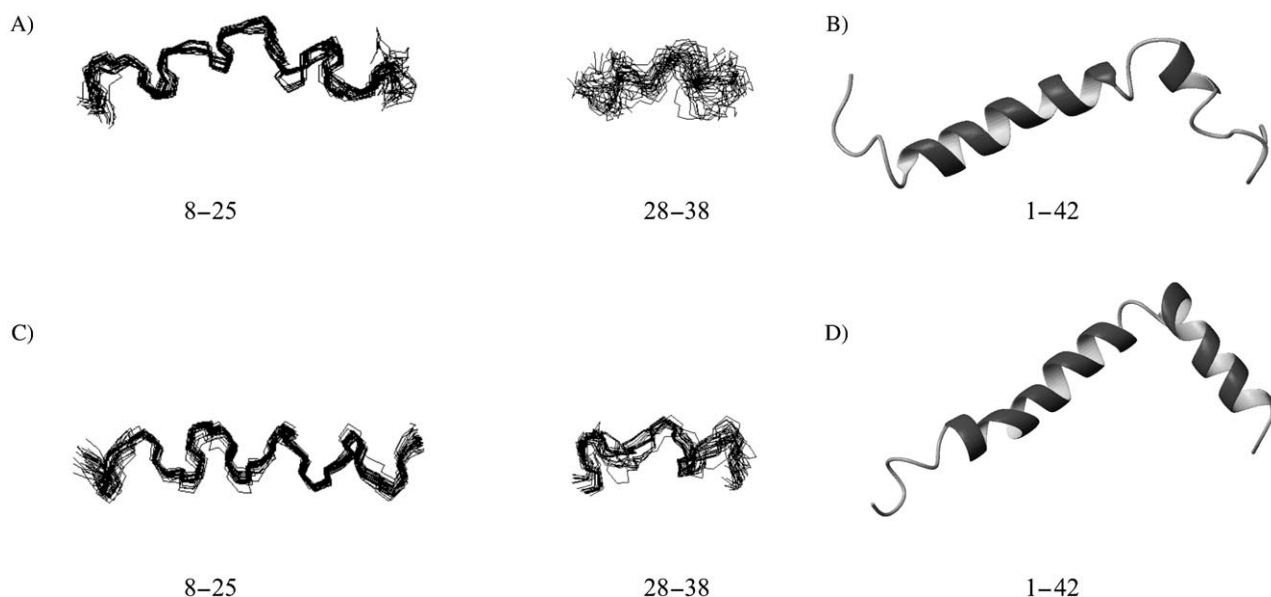
40 ns at 300 and 340 K.[10] This structure was fully immersed in a box of explicit water by using the simple-point-charge (SPC) model.[30] Analysis of the trajectories, performed by using the programs included in the GROMACS package as well as some

Figure 5. Comparison of Aβ-(1–42) structures in HFIP/H$_2$O 30:70 and 80:20 mixtures. A) Ensemble of the best ten Aβ-(1–42) structures in HFIP/H$_2$O 30:70 after AMBER minimization: regions 8–25 (left) and 28–38 (right). B) Ribbon representation of the whole Aβ-(1–42) structure in HFIP/H$_2$O 30:70. C) Ensemble of the best ten Aβ-(1–42) structures in HFIP/H$_2$O 80:20, taken from Crescenzi et al.:[10] regions 8–25 (left) and 28–38 (right). D) Ribbon representation of the whole Aβ-(1–42) structure in HFIP/H$_2$O 80:20, taken from Crescenzi et al.[10]

Table 1. Structural statistics of Aβ-(1–42) in HFIP/H$_2$O 30:70 and 80:20 (*v/v*) mixtures.

	HFIP/H$_2$O 30:70	HFIP/H$_2$O 80:20
NOE		
all	426	413
intraresidue	238	130
sequential	108	149
medium range	80	134
RMSD [Å]		
all backbone	4.89	1.97
N helix[a]	1.67	0.37
C helix[b]	2.86	0.59
Ramachandran		
most favored	47%	63%
additionally favored	40%	31%
generously favored	11%	5%
disallowed	3%	1%

[a] N helix corresponds to the 8–25 region for HFIP/H$_2$O 80:20 and the 10–23 region for HFIP/H$_2$O 30:70, respectively; [b] C helix corresponds to the 28–38 region of the peptide in both mixtures.

not shown). Throughout the simulation it was possible to observe the appearance of a strip perpendicular to the diagonal; this is indicative of the formation of an antiparallel β sheet made of the two β strands that contain amino acids 18–22 and 37–41.

In summary, as shown in Figure 6, at 300 K, time evolution corresponds to the partial loss of helicity experienced by Aβ-(1–42) when it is transferred from mostly organic to mostly aqueous HFIP/H$_2$O mixtures. Snapshots at 340 K that correspond to a more severe destabilization clearly indicate that residual, short helical segments evolve to stretches of β-structure that eventually pack into an antiparallel β sheet.

Discussion

The central role of Aβ-(1–42), which is the main peptide produced in vivo by β-amyloid precursor protein (APP) proteolysis, in Alzheimer's disease is well documented. However, whether the pathology is induced by soluble forms or is linked to deposits of fibrillar aggregates is still under debate. In vivo, the peptide is supposed to be helical when it is part of the precursor protein—since its sequence encompasses the single transmembrane domain of APP—and to have a β conformation in the plaques. Despite the impressive number of experimental studies, the molecular entity that causes neurotoxicity is still controversial. However, increasing evidence suggests that a conformational transition is the crucial step that determines the fate of Aβ-(1–42) under physiological or pathological conditions.

Many conformational studies have documented that, depending on the solvent features, the peptide can also undergo a conformational transition in vitro; since its conformation is strongly influenced by the environment.[31] This aspect seems to be a general feature of the peptide not only in solution but even in the solid state.[32] By using an integrated approach of experimental and theoretical methods, we have in this work tried to follow and describe, with as much structural detail as possible, the conformational transitions of Aβ-(1–42) when transferred from a very apolar to a fully polar medium. This path may be compared to a hypothetical physiological journey by the precursor protein towards the extracellular fluid.

The conformational steps uncovered along this path by using CD and NMR spectroscopy can be summarized as follows. The starting point was the high-resolution structure of Aβ-(1–42) in apolar environments, which was determined by Crescenzi et al.[10] in HFIP/H$_2$O. It was characterized by the terti-

D. Picone et al.
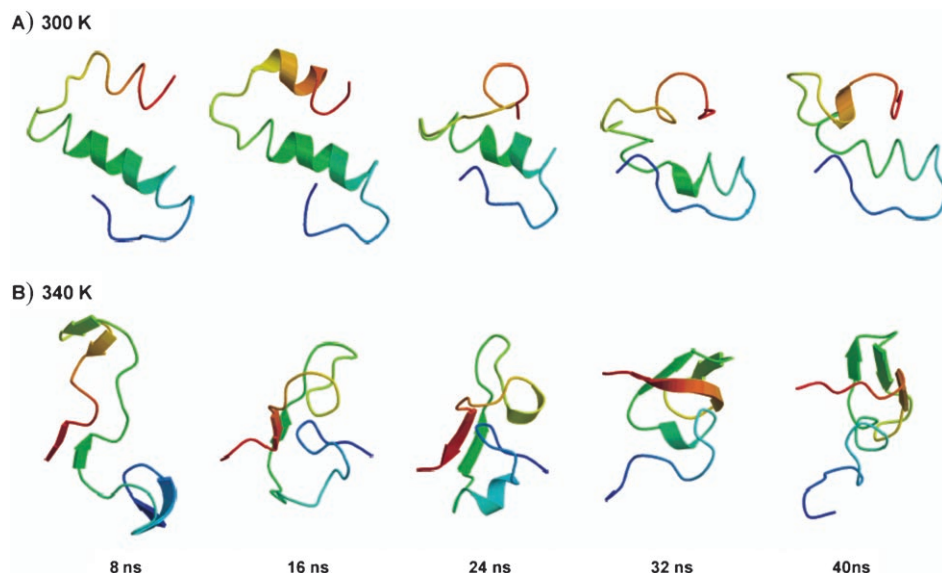
Figure 6. Aβ-(1–42) snapshots from A) 300 K and B) 340 K MD simulations in water. The figures were generated by using Molscript[55] and Raster3D.[56]

ary structure of two helical traits—a long, very regular one between residues 8 and 25 and a shorter, less regular one, from 28 to 38—that were connected by a β turn centered on residues 25–26 (Table 1). This tertiary structure is stable in mixtures with high percentages of organic component, from 90 to approximately 50 % HFIP.[10] When the water content of the mixtures was raised above 50 %, the tertiary structure was lost, whereas most of the secondary structure was retained even in mixtures in which water predominated. The NMR structure solved in HFIP/H$_2$O 30:70 (*v/v*) showed that the only secondary structures that were lost on going from a very apolar to an essentially polar environment were the β turn around residues 25–26 and, partially, the short C-terminal helix (Table 1; Figure 5). This finding is consistent with the central role recently attributed to the 25–35 core sequence[21] as a key motif in the α-to-β conformational transition. It is remarkable that, as shown by CD (Figure 1) and NMR spectroscopy (Figures 3, Figure 4), the peptide remained prevalently helical even in media that contained as much as 80 % water (*v/v*). The transition from α to β conformations occurred very sharply in media that comprised between 80 and 90 % water (Figure 1).

Owing to inherent limitations of the experimental techniques, it was not possible to describe β structures that were stable in 90–99 % water at the atomic level by using CD or NMR spectroscopy. However, it proved possible to make reasonable predictions on the basis of MD calculations. Analysis of long MD runs in explicit water at 300 K showed that it is possible to reproduce the experimental path of Aβ-(1–42) very accurately. In the MD runs, the first segment of secondary structure that lost regularity was also the β turn around residues 25–26, followed by the C-terminal helix. This is consistent with the experimental observations described above. The longer N-terminal helix, however, remained stable throughout. Short of trying to reproduce the conformational path by a

much longer (and costly) simulation, we introduced a disturbance by slightly raising the temperature. At 340 K, we observed the appearance of a small β sheet that was formed by two small distal β strands located in regions that previously hosted the two helices. This could represent the initial step of an aggregation process that leads to fibril assembly.

The β conformation can be stable in solutions that contain 90–99 % water. This is not the only outstanding feature of Aβ-(1–42) in HFIP/H$_2$O mixtures. Even more remarkable is the stability of the β conformations in solution for extended periods of time and the reversible nature of the α-to-β transition. We have shown that even starting from solutions that contain as much as 99 % water, addition of appropriate amounts of HFIP turns the peptide conformation back from β to α; this reversion of β aggregates occurs slowly but unequivocally. It is likely that these unusual features of Aβ-(1–42) in HFIP/H$_2$O are due in part to the presence of tightly bound HFIP molecules on the surface of the peptide. These bulky amphipatic molecules can act in a manner that is analogous to the isoleucine of the hYAP WW domain,[33] which covers an exposed hydrophobic surface and thereby stabilizes the short β structure of the domain. That is, a few HFIP molecules might "seal" the end of the short, initially paired β strands by protecting them from the aqueous environment. In addition, the role of these "sealing" molecules might be crucial in ensuring the reversibility of the α-to-β transition. Should the presence of a very small number of tightly bound HFIP molecules be the only cause of β-conformation stability and reversibility in Aβ-(1–42), it would be difficult to attribute biological significance to the observed conformational transitions. However, it is fair to say that these molecules can only slightly enhance native conformational tendencies. The coexistence of monomeric and oligomeric species in equilibrium has been recently demonstrated both for solutions of Aβ(1–40) peptide[34] and Pi3K-SH3 domain.[35] These works raise the question of whether the structure we determined for Aβ(1–42) in 70 % water could also reflect the structure of oligomers. In principle, if our NOEs partly reflect the fibrillar state, and thus represent trNOEs, we might perform the structural calculations as an ensemble calculation. However, this type of calculation requires more restraints than those required for a single static conformation, whereas we observe a smaller number of structurally relevant NOEs than for the NMR structure in 20 % water (Table 1). Besides, the solution conditions of both quoted works[34, 35] have been optimized to allow the study of intermediates. Our solution conditions for the NMR experiments

were selected with the aim of allowing high concentrations of monomeric Aβ(1–42) in solution. The range of solution conditions in our work in which chemical exchange might play a key role corresponds to the α-to-β conformational transition, that is from 20:80 to 1:99 HFIP/H_2O. The conformational equilibria in this range could be investigated by MD simulations, but introducing oligomers in these calculations would imply an arbitrary choice of a specific model for the oligomer. Accordingly, we refrained from any attempt to quantify the amount and nature of oligomers, although we could detect their presence indirectly.

The experimental observation that it is possible to turn Aβ-(1–42) β structures back to α-helical conformations is consistent with an increasing body of experimental evidence that suggests soluble oligomers might actually represent the true toxic form(s) of Aβ peptides.[8,9,36] Models representing several possible structures of aggregated forms have been proposed very recently. These range in size from dimers to 200-mer spherical β-balls;[13] but aggregation of helical peptides is a widespread mechanism—from antibiotic peptides to virus fusion peptides—that leads to membrane poration.

Furthermore, the finding that, under certain circumstances, aggregates can recover an α-helical conformation hints that a membrane-mediated activity of Aβ peptides could be a crucial step in the events that lead to neuronal death. This hypothesis is supported by the similarity of the Aβ-(1–42) structure in an apolar environment to the fusion domain of influenza hemagglutinin, by the ability of the Aβ C-terminal region to induce vesicle fusion,[37] and by the observation that it can enhance infection of several viruses at the stage of attachment or entry into the cell.[38] At the moment, attempts to identify regions of peptide that, prompted by the surrounding medium, drive conformational transitions still represents a promising approach to understanding the molecular basis of Alzheimer's disease. In addition, the structural characterization of a partially folded intermediate in the α-to-β transition and vice versa, opens many perspectives for the design of molecules that are able to interfere with the aggregation process. This has great potential for possible therapeutic applications.

Experimental Section

Sample preparation: Aβ-(1–42) was synthesized by using standard solid-phase synthesis techniques[39] with a Milligen 9050 synthesizer, as described in detail by Crescenzi et al.,[10] and purified by HPLC according to published methods.

Unstructured aggregates, which are often present in untreated samples from synthesis experiments, can severely hamper solubility. To disaggregate such material, which can be present in the dry peptide, all CD and NMR samples were treated with trifluoroacetic acid (TFA) immediately before being dissolved in the final mixture, as described by Jao et al. [40] Unless otherwise stated, the solvent composition of all HFIP/H_2O mixtures is reported as volume ratio.

CD spectroscopy and analysis: All CD spectra were recorded on a JASCO J-715 spectropolarimeter equipped with a thermostated cell holder, by using a quartz cell of 0.1 cm path length.

Spectra were recorded over the wavelength range of 260–190 nm with a bandwidth of 2.0 nm and a time constant of 8.0 s, at 25 °C. Spectra were corrected for the contribution of the solvent. Unless otherwise stated, peptide concentration of about 16 μM was used in all experiments. Final concentrations were achieved by dissolving the TFA-treated peptide in neat HFIP and then by adding the appropriate amount of premixed HFIP/H_2O up to the needed solvent composition. The following HFIP/H_2O mixtures were analyzed: 80:20, 40:60, 30:70, 20:80, 15:85, 10:90, 1:99.

A series of CD spectra were analyzed in terms of helical and β-conformation content by using the software package CDPRO.[23] The programs CONTIN and CDSSTR (part of CDPro) were used to analyze the 40:60, 30:70, 20:80, 15:85, 10:90 CD spectra by using the SP43 protein reference set. The resulting spectra were used to fit the experimental spectra to a linear combination of the CONTIN and CDSSTR spectra within the Origin Software package (Origin-Lab, Northampton, MA, USA). This analysis provided the most accurate estimation of helical, β, turn, and unordered conformations for the peptide in different water fractions.

NMR spectroscopy and structure calculations: NMR samples were prepared by dissolving the dry peptide in 50% of the total required amount of [D_2]HFIP and subsequently adding the remaining amount of solvent as a mixture [D_2]HFIP/H_2O. All mixtures were analyzed by CD and NMR spectroscopy. Spectra were acquired at 300 K on Bruker DRX-400, DRX-500, and DRX-600 spectrometers (Naples, Italy), and on Bruker DRX-750 and DRX-600 spectrometers (Utrecht, The Netherlands). Unless otherwise stated, the peptide concentration was 1 mM. TOCSY[41] and NOESY[42] spectra were collected in the phase-sensitive mode by using quadrature detection. The water signal was suppressed by low-power selective irradiation. Typical data sizes were 2048 addresses in $t2$ and 512 equidistant $t1$ values (1024 in the spectra acquired at 750 MHz). Mixing times were 150 ms in the NOESY experiments and 80 ms in the TOCSY experiments. All spectra were processed by using NMRPipe[43] and analyzed by using NMRView.[44] Chemical shifts were referenced to the residual HFIP signal at 3.88 ppm.

Based on the natural abundance of ^{13}C, ^{13}C-HSQC experiments were also acquired with the samples in the HFIP/H_2O mixtures with a ratio 30:70 and 80:20. Experiments were collected in phase-sensitive mode[45,46] by using water gradient suppression. The data sizes were 1024 in $t2$ and 400 in $t1$ values. For each experiment 160 scans were made. The chemical shifts of the carbons were referenced to the CH value of the HFIP at 71 ppm.[47]

Sequential assignment was achieved by using standard NOE connectivity-based protocol.[26]

Most peaks in the NOESY spectra, except those that showed spectral overlap were unambiguously assigned. NOE cross-peaks were integrated with NMRView and were converted into upper-distance bounds with routine CALIBA of the package DYANA.[48] The final list included 238 intraresidue, 108 sequential, and 80 medium range NOEs. These were used to generate an ensemble of 100 structures by the standard protocol of simulated annealing in torsion-angle space, which was implemented with DYANA by using 6000 steps. No dihedral or hydrogen bond restraints were used.

The final structures were analyzed by using the program MOLMOL.[49]

MD simulations: These were performed with GROMACS,[28,29] by using the GROMOS96 43A1 force field.[50] The simulations were run for 40 ns at 300 and 340 K by starting from the representative NMR structure that was determined in HFIP/H_2O 80:20. The struc-

tures were fully immersed in explicit water by using the SPC model.[30] Analysis of the trajectories was performed by using programs included in the GROMACS package as well as some in-house scripts.

The peptide was solvated in a cubic box of explicit water with a minimum solute-box distance of 14 Å. Three sodium counter ions were added in each case to electroneutralize the system. The system comprised 17 250 SPC molecules, corresponding to a total number of 52 162 atoms. Periodic boundary conditions were applied. Each system was first energy minimized by using 1000 steps of Steepest Descent (SD) algorithm.

The equilibration of each system was performed in five 20 ps phases during which the force constant of the position-restraints term for the solute was decreased from 1000 to 0 kJ mol^{-1} nm^{-2} (1000, 1000, 100, 10, 0 kJ mol^{-1} nm^{-2}, respectively). The initial velocities were generated at the desired temperatures by following a Maxwellian distribution. All simulations were performed in the NPT ensemble by weakly coupling the system to external temperature and pressure baths,[51] except for the first 20 ps equilibration which was performed at constant volume (NVT).

A 4 fs time step was used for the leapfrog algorithm integration. The LINCS algorithm[52] was used for bond-length constraining in conjunction with dummy atoms for the aromatic rings and amino group in the side chains.[53] This allowed the use of the longer integration-time step of 4 fs. Peptide, solvent(s), and counter ions were coupled separately to a temperature bath with a time constant of 0.1 ps. The pressure was coupled to an external bath at 1 bar with a time constant of 0.5 ps and a compressibility of 4.5× 10^{-5} bar^{-1} for simulations in water. Periodic-boundary conditions were applied throughout the simulation. A twin-range cut-off of 0.8 and 1.4 nm was used for nonbonded interactions. The generalized reaction field[54] was used with a dielectric constant of 54 beyond the 1.4 nm cut off. The nonbonded pair list was updated every five MD steps.

All simulations were performed in parallel with four processors on a LINUX cluster (1.3 MHz Athlon processors) by using the parallel version of GROMACS. As a central processing unit (CPU) cost indication, 1 ns took about 30 h.

PDB ID code: The coordinates have been deposited in the PDB with the ID 1Z0Q.

Acknowledgements

Keywords: Alzheimer's disease · circular dichroism · fibrils · molecular dynamics · NMR spectroscopy

[1] L. L. Iversen, R. J. Mortishire-Smith, S. J. Pollack, M. S. Shearman, *Biochem. J.* **1995**, *311*, 1–16.
[2] M. Arrasate, S. Mitra, E. S. Schweitzer, M. R. Segal, S. Finkbeiner, *Nature* **2004**, *431*, 805–810.
[3] P. A. Temussi, L. Masino, A. Pastore, *EMBO J.* **2003**, *22*, 355–361.
[4] E. Terzi, G. Holzemann, J. Seelig, *J. Mol. Biol.* **1995**, *252*, 633–642.5.
[5] S. Varadarajan, S. Yatin, M. Aksenova, D. A. Butterfield, *J. Struct. Biol.* **2000**, *130*, 184–208.
[6] D. M. Walsh, I. Klyubin, J. V. Fadeeva, W. K. Cullen, R. Anwyl, M. S. Wolfe, M. J. Rowan, D. J. Selkoe, *Nature* **2002**, *416*, 535–539.
[7] R. Kayed, E. Head, J. L. Thompson, T. M. McIntire, S. C. Milton, C. W. Cotman, C. G. Glabe, *Science* **2003**, *300*, 486–489.
[8] J. P. Cleary, D. M. Walsh, J. J. Hofmeister, G. M. Shankar, M. A. Kuskowski, D. J. Selkoe, K. H. Ashe, *Nat. Neurosci.* **2005**, *8*, 79–84.
[9] A. Demuro, E. Mina, R. Kayed, S. C. Milton, I. Parker, C. G. Glabe, *J. Biol. Chem.* **2005**, *280*, 17 294–17 300.
[10] O. Crescenzi, S. Tomaselli, R. Guerrini, S. Salvadori, A. M. D'Ursi, P. A. Temussi, D. Picone, *Eur. J. Biochem.* **2002**, *269*, 5642–5648.
[11] S. K. Rhee, A. P. Quist, R. Lal, *J. Biol. Chem.* **1998**, *273*, 13 379–13 382.
[12] H. Lin, R. Bhatia, R. Lal, *FASEB J.* **2001**, *15*, 2433–2444.
[13] D. V. Laurents, P. M. Gorman, M. Guo, M. Rico, A. Chakrabartty, M. Bruix, *J. Biol. Chem.* **2005**, *280*, 3675–3685.
[14] J. P. Lee, E. R. Stimson, J. R. Ghilardi, P. W. Mantyh, Y.-A. Lu, A. M. Felix, W. Llanos, A. Behbin, M. Cummings, M. Van Criekinge, W. Timms, J. E. Maggio, *Biochemistry* **1995**, *34*, 5191–5200.
[15] J. Jarvet, P. Damberg, K. Bodell, L. E. G. Eriksson, A. Gräslund, *J. Am. Chem. Soc.* **2000**, *122*, 4261–4268.
[16] S. Zhang, K. Iwata, M. J. Lachenmann, J. W. Peng, S. Li, R. R. Stimson, Y. A. Lu, A. M. Felix, J. E. Maggio, J. P. Lee, *J. Struct. Biol.* **2000**, *130*, 130–141.
[17] R. Riek, P. Güntert, H. Döbell, B. Wipf, K. Wüthrich, *Eur. J. Biochem.* **2001**, *268*, 5930–5936.
[18] C. J. Barrow, M. G. Zagorski, *Science* **1991**, *253*, 180–182.
[19] H. Sticht, P. Bayer, D. Willbold, S. Dames, C. Hilbich, K. Beyreuther, R. W. Frank, P. Roesch, *Eur. J. Biochem.* **1995**, *233*, 293–298.
[20] T. Kohno, K. Kobayashi, T. Maeda, K. Sato, A. Takashima, *Biochemistry* **1996**, *35*, 16 094–16 104.
[21] A. M. D'Ursi, M. R. Armenante, R. Guerrini, S. Salvadori, G. Sorrentino, D. Picone, *J. Med. Chem.* **2004**, *47*, 4231–4238.
[22] L. Otvos, G. I. Szendrei, V. M. Lee, H. H. Mantsch, *Eur. J. Biochem.* **1993**, *211*, 249–257.
[23] N. Sreerama, R. W. Woody, *Anal. Biochem.* **2000**, *287*, 252–260.
[24] C. J. Barrow, A. Yasuda, P. T. M. Kenny, M. G. Zagorski, *J. Mol. Biol.* **1992**, *225*, 1075–1093.
[25] Y. Fezoui, D. B. Teplow, *J. Biol. Chem.* **2002**, *277*, 36 948–36 954.
[26] K. Wüthrich, *NMR of Proteins and Nucleic Acids*, Wiley, New York, **1986**, pp. 162–175.
[27] D. S. Wishart, B. D. Sykes, *Methods Enzymol.* **1994**, *239*, 363–392.
[28] H. J. C. Berendsen, D. van der Spoel, R. van Drunen, *Comput. Phys. Commun.* **1995**, *91*, 43–56.
[29] E. Lindahl, B. Hess, D. van der Spoel, *J. Mol. Model.* **2001**, *7*, 306–317.
[30] H. J. C. Berendsen, J. P. M. Postma, W. F. van Gunsteren, J. Hermans in *Intermolecular Forces* (Ed.: B. Pullman), Reidel, Dordrecht, **1981**, pp. 331–342.
[31] A. B. Clippingdale, J. D. Wade, C. J. Barrow, *J. Pept. Sci.* **2001**, *7*, 227–249.
[32] A. T. Petkova, R. D. Leapman, Z. Guo, W. M. Yau, M. P. Mattson, R. Tycko, *Science* **2005**, *307*, 262–265.
[33] M. J. Macias, M. Hyvonen, E. Baraldi, J. Schultz, M. Sudol, M. Saraste, H. Oschkinat, *Nature* **1996**, *382*, 646–649.
[34] S. Narayanan, B. Reif, *Biochemistry* **2005**, *44*, 1444–1452.
[35] N. Carulla, G. L. Caddy, D. R. Hall, J. Zurdo, M. Gairi, M. Feliz, E. Giralt, C. V. Robinson, C. M. Dobson, *Nature* **2005**, *436*, 554–558.
[36] M. P. Lambert, . A. K. Barlow, B. A. Chromy, C. Edwards, R. Freed, M. Liosatos, T. E. Morgan, I. Rozovsky, B. Trommer, K. L. Viola, P. Wals, C. Zhang, C. E. Finch, G. A. Krafft, W. L. Klein, *Proc. Natl. Acad. Sci. USA* **1998**, *95*, 6448–6453.
[37] T. Pillot, M. Goethals, B. Vanloo, C. Talussot, R. Brasseur, J. Vandekerckhove, M. Rosseneu, L. Lins, *J. Biol. Chem.* **1996**, *271*, 28 757–28 765.
[38] W. M. Wojtowicz, M. Farzan, J. L. Joyal, K. Carter, G. J. Babcock, D. I. Israel, J. Sodroski, T. Mirzabekov, *J. Biol. Chem.* **2002**, *277*, 35 019–35 024.

[39] E. Atherton, R. C. Sheppard, *Solid Phase Peptide Synthesis: A Practical Approach*, IRL, Oxford, **1989**, pp. 25–53.

[40] S. C. Jao, K. Ma, J. Talafous, R. Orleo, M. G. Zagorski, *Int. J. Exp. Clin. Invest.* **1997**, *4*, 240–252.

[41] A. Bax, D. G. Davis, *J. Magn. Reson.* **1985**, *65*, 355–360.

[42] J. Jeener, B. H. Meyer, P. Bachman, R. R. Ernst, *J. Chem. Phys.* **1979**, *71*, 4546–4553.

[43] F. Delaglio, S. Grzesiek, G. Vuister, G. Zhu, J. Pfeifer, A. Bax, *J. Biomol. NMR* **1995**, *6*, 277–293.

[44] B. A. Johnson, R. A. Blevins, *J. Biomol. NMR* **1994**, *4*, 603–614.

[45] L. E. Kay, P. Keifer, T. Saarinen, *J. Am. Chem. Soc.* **1992**, *114*, 10663–10665.

[46] J. Schleucher, M. Schwendinger, M. Sattler, P. Schmidt, O. Schedletzky, S. J. Glaser, O. W. Sorensen, C. Griesinger, *J. Biomol. NMR* **1994**, *4*, 301–306.

[47] K. Yoshida, T. Yamaguchi, T. Adachi, T. Otomo, D. Matsuo, T. Takamaku, N. Nishi, *J. Chem. Phys.* **2003**, *119*, 6132–6142.

[48] P. Güntert, C. Mumenthaler, K. Wüthrich, *J. Mol. Biol.* **1997**, *273*, 283–298.

[49] R. Koradi, M. Billeter, K. Wüthrich, *J. Mol. Graphics* **1996**, *14*, 51–55.

[50] X. Daura, A. E. Mark, W. F. van Gunsteren, *J. Comput. Chem.* **1998**, *19*, 535–547.

[51] H. J. C. Berendsen, J. P. M. Postma, A. Di Nola, J. R. Haak, *J. Chem. Phys.* **1984**, *81*, 3684–3690.

[52] B. Hess, H. Bekker, H. J. C. Berendsen, J. G. E. M. Fraaije, *J. Comput. Chem.* **1997**, *18*, 1463–1472.

[53] K. A. Feenstra, B. Hess, H. J. C. Berendsen, *J. Comput. Chem.* **1999**, *20*, 786–798.

[54] I. G. Tironi, R. Sperb, P. E. Smith, W. F. van Gunsteren, *J. Chem. Phys.* **1995**, *102*, 5451–5459.

[55] P. J. Kraulis, *J. Appl. Crystallogr.* **1991**, *24*, 946–950.

[56] E. A. Merrit, M. E. P. Murphy, *Acta Crystallogr. Sect. D Biol. Crystallogr.* **1994**, *50*, 869–873.